# A Fiber Bragg Grating Strain Sensor-based Glove to Accurately Measure the Bend Angle of the Finger Flexed at the Proximal Interphalangeal Joints

Chandan Kumar Jha, Arup Lal Chakraborty
Electrical Engineering, Indian Institute of Technology Gandhinagar, Gandhinagar, India
chandan.kumar.jha@iitgn.ac.in

***Abstract*—Accurate measurement of finger joint angles is very important in the fields such as rehabilitation, bionics, etc. In this paper, we present a fiber Bragg grating (FBG) sensor-based flexure sensing glove to measure the finger joint angles with high accuracy. We evaluate its accuracy and repeatability on four human subjects by measuring their proximal interphalangeal (PIP) joint angles of the index, middle and the ring fingers. Our glove showed excellent agreement (R-Squared: 0.9985) with the inertial measurement unit (IMU) sensor readings. The glove outperforms several existing sensors exhibiting a maximum error (1.42 degrees), mean error (0.45 degrees) and maximum standard deviation (0.56 degrees). In the future, the study will be extended to all the joints.**

***Keywords—fiber Bragg grating; flexure sensor; rehabilitation; instrumented glove***

## I. Introduction

The human hand is a very complex anatomical structure with up to 27 degrees of freedom. Each finger consists of three phalanges namely, proximal, middle and the distal phalanges. The thumb does not have the middle phalange. The closest joint from the palm called as metacarpophalangeal joint (MCP) is the largest finger joint. The MCP joint is followed by the PIP and the distal interphalangeal joint (DIP) respectively. Areas such as physical rehabilitation, bionics, etc. require accurate and precise measurement of finger joint angles. But due to complex articulation and small area available on the hand, developing sensors for accurate joint measurement becomes a challenging task. In the past, several sensorized gloves [1]–[13] have been proposed employing different sensors like resistive flex sensors [2]–[5], magnetic sensors [6]–[9], optical sensors [10]–[13], etc. The widely used resistive sensors have signal drift issues, poor repeatability and require tedious calibration procedures [5]. Magnetic sensors such as Hall-effect sensors are susceptible to nearby magnetic fields. In this paper, we demonstrate an FBG-based flexure sensing glove to measure the finger joint angles with very high accuracy and precision. We study the accuracy and repeatability of our glove by measuring the PIP joint angles of three different fingers of four human subjects. FBG sensors were chosen due to their very high strain sensitivity (1.2 pm/$\mu\epsilon$), small footprint and immunity to electromagnetic interference. FBGs are constructed by periodically modulating the refractive index of the core of a photosensitive optical fiber. When light is launched into the fiber, a narrow band of light centered on the Bragg wavelength is reflected that is proportional to the strain applied to the FBG. The Bragg wavelength is sensitive to the axial strain applied to the FBG. The value of the applied strain can, therefore, be calculated by accurately measuring the shift in the Bragg wavelength.

## II. Sensor Construction

In this work, three FBG based sensor units were attached on a glove, shown in fig. 1a, to measure the three PIP joint angles of the index, middle and the ring finger respectively. Three IMU sensors were also placed on the phalanges to compare the sensor performance. A spring with stiffness constant of 100 $Nm^{-1}$, wire diameter of 0.2 mm, outer diameter of 1.9 mm and length 10 mm was attached to an acrylate SMF-28 FBG to construct the sensor unit. The FBGs used had the central wavelength of 1530.069 nm, 1530.115 nm and 1530.178 nm, the bandwidth of 0.20 nm, 0.33 nm and 0.27 nm and reflectivity of 94%, 97%, and 93% respectively. The spring side of the sensor is fixed on the dorsal side of the palm as shown in fig. 1b. The other end is tied to the phalanges following the joint of interest. Flexing of the finger causes the displacement (d) of the fiber due to spring elongation and is given by $d = h\theta$, where h is the radius of the finger joint, and $\theta$ is the joint angle. Strain introduced in the FBG is proportional to this displacement. Therefore the joint angle can be calculated from the Bragg wavelength shift of the FBG.

## III. Experimental Setup

An interrogation system based on tunable diode laser spectroscopy technique was designed to interrogate the FBG sensors. The details of the system have been described in [14]. Fig. 2a shows the schematic diagram of the interrogation system. A narrow line-width fiber coupled 1531.52 nm distributed feedback (DFB) laser (Toptica Photonics, LD-1550-0040-DFB-1) was used as the light source. A laser temperature controller (ThorLabs, TED 200C) and current controller (ThorLabs, LDC 220C) were used to tune the emission wavelength of the laser. Two fixed-gain photo-detectors (ThorLabs, PDA10D-EC), a 1x2 optical switch (Lightwave Link, 1-2-L-9-L-3) and a 2x2 optical switch (Lightwave Link, 2-2-L-9-L-3) were used together to detect the light from the FBGs, the Mach-Zehnder interferometer (MZI) and the gas-cell. In this technique, the MZI transmission peaks (pink trace in fig. 2b) is used as a frequency scale to measure the frequency shift of the FBG reflected spectrum. The normalized gas-line (solid black trace in fig. 2b) is then used

978-1-5386-4707-3/18/$31.00 ©2018 IEEE

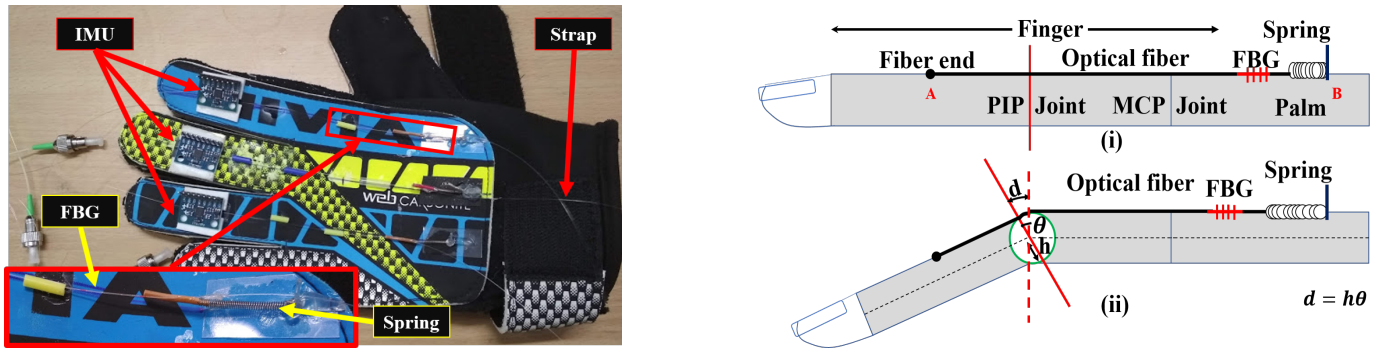


(a) (b)

Fig. 1. (a) Placement of the sensors on the index, middle and the ring finger of the glove to measure the PIP joint angles; (b) The schematic diagram of the sensor design - (i) Initial position of the finger, (ii) Flexed finger (causes the spring to elongate).

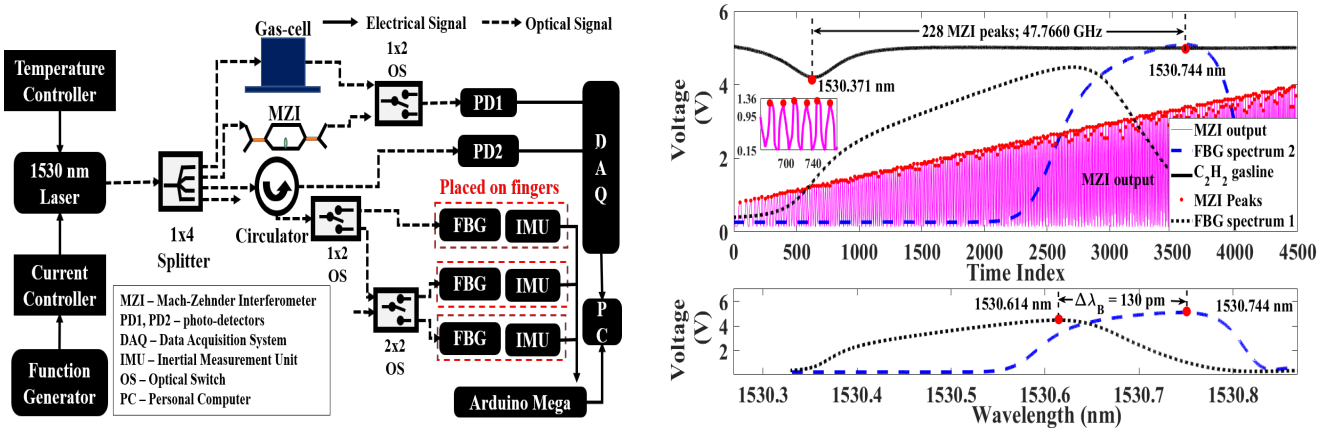


(a) (b)

Fig. 2. (a) Experimental setup; (b) Wavelength referencing of FBG spectrum using the normalized acetylene ($C_2H_2$) gas-line and the MZI transmission peaks; inset shows the zoomed view of the MZI output. FBG spectrum 1 and 2 are the reflected spectra obtained for two different values of strain. The normalized gas-line has been offset by 5 volts for clear representation. The subplot below shows the wavelength referenced FBG spectra.

as an absolute wavelength reference to convert the frequency shifts to wavelength shifts. A 16-bit data acquisition system (Measurement Corp USA, USB-1608G) was used to digitize the photo-detector signals with a sampling rate of 250 kS/s. IMU sensors (InvenSense, MPU6050) connected to Arduino Mega 2560 were used to measure the joint angles. In the experiments, the IMU sensor readings were considered to be the true measure of the joint angles. The angle measurements from our sensor were compared with the IMU readings. In a separate experiment, the accuracy and repeatability of the IMU sensor were determined using a 0.08° resolution bevel protractor. The IMU sensor demonstrated very small mean error (0.43°) and standard deviation (0.63°) and therefore was chosen as a reference.

The FBG reflected spectrum was acquired by first tuning the lasing wavelength close to the FBG resonance by adjusting the laser temperature and then varying the laser current with a 50 Hz periodic current ramp (30 mA - 250 mA) to repeatedly scan the emission wavelength across the FBG resonance. The frequency shift of the FBG reflected spectrum was calculated by multiplying the number of MZI peaks traversed by the spectrum (228 as shown in the figure 2b) with the free spectral range of the MZI (0.2095 GHz). The 1530.371 nm acetylene gas absorption line was used to convert the frequency shifts (47.7660 GHz) to wavelength shifts (373 pm). This method of wavelength referencing has been widely used in tunable laser diode spectroscopy techniques [15]. The gasline and the MZI transmission spectrum are very stable over time and need not be acquired frequently [15]. Therefore, they were acquired only once at the start of the experiments. Fig. 2b shows the normalized acetylene (1530.371 nm) gas-line (solid black trace) and the MZI transmission peaks (pink trace) used to wavelength reference the FBG reflected spectra. In the figure, FBG spectrum 1 and 2 were obtained while the FBG was subjected to two different amounts of strain. In the subplot below, the wavelength-referenced spectra of the FBG (dotted black trace and dashed blue trace) have been shown. The wavelength shift (130 pm) of the FGB spectrum 2 with respect to the FBG spectrum 1 can be calculated by subtracting the Bragg wavelength of FBG spectrum 1 (1530.614 nm) from that FBG spectrum 2 (1530.744 nm).

## IV. Experimental Methods

The subjects wore the glove on the left hand and rested the hand comfortably on an experimental table. First, the subject bent the index finger at the PIP joint continuously at a very slow speed of about 0.5° per second. The movement of the other fingers was restricted by holding the fingers down

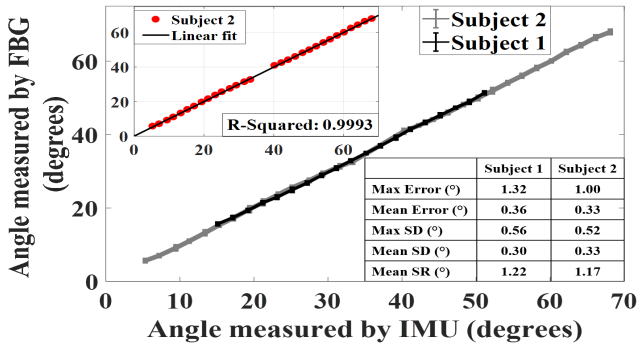


(a)

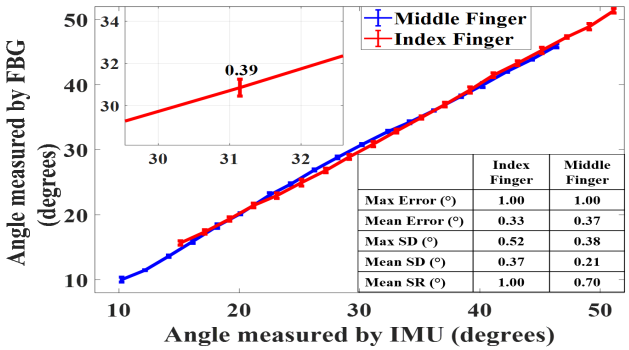


(b)

Fig. 3. (a) PIP joint angle of the index finger of subject 1 and 2 measured by the FBG sensor; (b) PIP joint angle of the middle and the index finger of subject 2 measured by the FBG sensor compared to the IMU sensor. The inset shows the zoomed view of the graph with the errorbar.

supported by the edge of the stage. A LabVIEW application recorded the IMU sensor values, and the FBG reflected spectrum at every 2° of rotation. A linear model was fitted to the IMU readings and the corresponding wavelength shifts. The model parameters were then used to compute joint angles from the wavelength shifts in subsequent runs. These parameters are used to calibrate the sensor. The experiment was repeated five times with a one-minute interval to test the repeatability, i.e., the variation in multiple measurements of the same joint angle. The procedure was repeated to measure the PIP joint angle of the other two fingers.

## V. Results

Fig. 3a shows the measurement of the PIP joint angle of the index finger of subject 1 and 2. Our sensor measurements showed excellent agreement with the IMU readings (R-Squared: 0.9993) as shown in the inset. The variation in readings over multiple runs of the experiment was very less (maximum standard deviation (SD): 0.56°) which shows that the sensor is precise and reliable. Subject 1 showed higher error, SD and statistical range (SR) values compared to subject 2 due to loose-fitting of the glove. Fig. 3b shows the angle measurement of the PIP joint of the index and the middle finger of subject 2. The mean and the maximum error from all the measurements of subject 2 were 0.35° and 1.01° respectively. The measurements from the index finger shows better agreement with IMU readings (R-Squared:0.9995) than that from the middle finger (R-Squared:0.9985). The performance of the glove on all of the four subjects has been summarized in Table I and compared with the earlier developed sensors. Our glove demonstrated a maximum error of 1.42°, mean SD of 0.37° and mean SR of 1.03° which are much better than the other sensors tabulated in the Table I.

A virtual reality game that could be played using the glove was developed using the Unity game development engine. The screen-shot of the game has been shown in fig. 4. Currently, the user can steer the paddle right and left by bending the index and the ring finger and fire the ball by bending the middle finger respectively. It will be further developed to be used for rehabilitation of stroke patients.

## VI. Conclusion

In this work, the performance of the FBG-based flexure sensor was evaluated on four human subjects with different hand features. Three FBG sensors were attached on a glove to simultaneously measure the PIP joint angles of the index, middle and the ring fingers respectively. The sensors exhibited very good accuracy (max error: 1.42°), high repeatability (mean SD: 0.37°), very good dynamic response and outperformed several earlier developed sensors. The results clearly show that our sensor is more accurate, precise and reliable than several other existing sensors which makes it a potential choice for developing sensorized gloves. In future, multiple sensors will be attached on the glove to measure all the joint angles simultaneously, and their interdependence will be studied. The efficacy of the glove and the game together will be tested as a rehabilitation system for stroke patients.

TABLE I
Maximum Error, SD and SR Values Obtained For Each Subject. The Mean Value Of The Results Have Been Compared To Values Reported For Earlier Existing Sensors.

| Subjects | Max Error (°) | SD (°) | SR (°) |
|---|---|---|---|
| 1 | 1.32 | 0.33 | 1.11 |
| 2 | 1.01 | 0.32 | 0.92 |
| 3 | 1.42 | 0.29 | 0.82 |
| 4 | 1.30 | 0.54 | 1.28 |
| **Mean values (our glove)** | **1.26** | **0.37** | **1.03** |
| Optical Polarizer [13] | 2.7 | - | - |
| FBG sensor [11] | 2.0 | - | - |
| HITEG-Glove [3] | - | 1.07 | 3.25 |
| HumanGlove [9] | - | 2.14 | 6.65 |

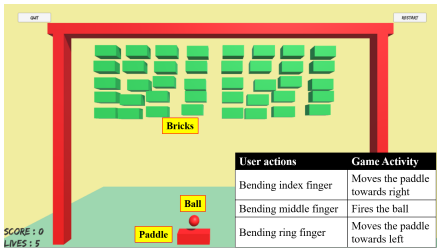


Fig. 4. Screenshot of the virtual reality game developed that can be played using the glove.

## VII. Acknowledgment

This research was supported by Visvesvaraya PhD Scheme.

## REFERENCES


[1] L. Dipietro, A. M. Sabatini, and P. Dario, "A survey of glove-based systems and their applications," *IEEE Transactions on Systems, Man and Cybernetics Part C: Applications and Reviews*, vol. 38, no. 4, pp. 461–482, 2008.

[2] G. Saggio, F. Riillo, L. Sbernini, and L. R. Quitadamo, "Resistive flex sensors: A survey," *Smart Materials and Structures*, vol. 25, no. 1, p. 13001, 2015. [Online]. Available: http://dx.doi.org/10.1088/0964-1726/25/1/013001

[3] G. Saggio, "A novel array of flex sensors for a goniometric glove," *Sensors and Actuators A: Physical*, vol. 205, pp. 119 – 125, 2014. [Online]. Available: http://www.sciencedirect.com/science/article/pii/S0924424713005451

[4] D. E. Nathan, M. J. Johnson, and J. R. McGuire, "Design and validation of low-cost assistive glove for hand assessment and therapy during activity of daily living-focused robotic stroke therapy," *J Rehabil Res Dev*, vol. 46, no. 5, pp. 587–602, 2009.

[5] N. W. Williams, J. M. T. Penrose, C. M. Caddy, E. Barnes, D. R. Hose, and P. Harley, "A goniometric glove for clinical hand assessment: Construction, calibration and validation," *The Journal of Hand Surgery: British & European Volume*, vol. 25, no. 2, pp. 200 – 207, 2000. [Online]. Available: http://www.sciencedirect.com/science/article/pii/S0266768199903601

[6] Y. Ma, Z. H. Mao, W. Jia, C. Li, J. Yang, and M. Sun, "Magnetic hand tracking for human-computer interface," *IEEE Transactions on Magnetics*, vol. 47, no. 5, pp. 970–973, May 2011.

[7] H. G. Kortier, J. Antonsson, H. M. Schepers, F. Gustafsson, and P. H. Veltink, "Hand pose estimation by fusion of inertial and magnetic sensing aided by a permanent magnet," *IEEE Transactions on Neural Systems and Rehabilitation Engineering*, vol. 23, no. 5, pp. 796–806, September 2015.

[8] C.-S. Fahn and H. Sun, "Development of a data glove with reducing sensors based on magnetic induction," *IEEE Transactions on Industrial Electronics*, vol. 52, no. 2, pp. 585–594, April 2005.

[9] L. Dipietro, A. M. Sabatini, and P. Dario, "Evaluation of an instrumented glove for hand-movement acquisition," *The Journal of Rehabilitation Research and Development*, vol. 40, no. 2, p. 181, 2003. [Online]. Available: http://www.rehab.research.va.gov/jour/03/40/2/PDF/dipietro.pdf

[10] K. Li, I. M. Chen, S. H. Yeo, and C. K. Lim, "Development of finger-motion capturing device based on optical linear encoder," *J Rehabil Res Dev*, vol. 48, no. 1, pp. 69–82, 2011.

[11] A. F. Da Silva, A. F. Goncalves, P. M. Mendes, and J. H. Correia, "FBG sensing glove for monitoring hand posture," *IEEE Sensors Journal*, vol. 11, no. 10, pp. 2442–2448, 2011.

[12] M. Nishiyama and K. Watanabe, "Wearable sensing glove with embedded hetero-core fiber-optic nerves for unconstrained hand motion capture," *IEEE Transactions on Instrumentation and Measurement*, vol. 58, no. 12, pp. 3995–4000, 2009.

[13] L. Wang, T. Meydan, and P. I. Williams, "A two-axis goniometric sensor for tracking finger motion," *Sensors (Switzerland)*, vol. 17, no. 4, 2017.

[14] A. Roy, A. L. Chakraborty, and C. K. Jha, "Fiber Bragg grating interrogation using wavelength modulated tunable distributed feedback lasers and a fiber-optic Mach Zehnder interferometer," *Applied optics*, vol. 56, no. 12, pp. 3562–3569, 2017.

[15] A. Upadhyay and A. L. Chakraborty, "Residual amplitude modulation method implemented at the phase quadrature frequency of a 1650-nm laser diode for line shape recovery of methane," *IEEE Sensors Journal*, vol. 15, no. 2, pp. 1153–1160, 2015.